Cross sections for ionization of metastable rare-gas atoms (Ne*, Ar*, Kr*, Xe*) and of metastable N_2^*,CO* molecules by electron impact*

D. Ton-That and M. R. Flannery
School of Physics, Georgia Institute of Technology, Atlanta, Georgia 30332
(Received 30 September 1976)

Cross sections for the collisional ionization of the metastable atoms Ne*, Ar*, Kr*, and Xe* by electrons with impact energy E in the range $6 < E < 250$ eV are determined in the Born and binary-encounter approximations. For low energies ϵ of ejection, the s-d and s-f bound-free transitions dominate the associated form factor, while transitions to continuum states with progressively higher angular momentum gain importance with increasing ϵ. While up to nine partial waves are normally sufficient for convergence of the bound-free form factor at a given energy ϵ and momentum change K of the ejected electron, as many as 30 are required for those K in the vicinity of the Bethe ridge at large ϵ. These properties are the origin of the overall closeness obtained between the Born and binary-encounter cross sections. Also inner-shell ionization, as described by the binary-encounter treatment, becomes increasingly important as the target atom becomes more complex. Cross sections for ionization of metastable N_2^* and CO* are also determined. Good agreement with available measurements (for Ne* and Ar*) is obtained.

I. INTRODUCTION

Apart from the Born and binary-encounter treatments for the ionization of metastable helium[1] by electron impact, little is known about the cross sections for ionization of metastable rare-gas atoms X (Ne*, Ar*, Kr*, Xe*) by electron impact. This information is important in the modeling and feasibility studies of certain excimer lasers. In particular, very recent observations[2-8] of high-power laser emission from a new class of molecules—the noble-gas monohalides (ArF*, KrF*, and XeF*, for example)—have demonstrated the potential of a new class of high-power high-efficiency and partially tunable lasers operating around 3000 Å. The lasing transition originates on an excited molecular state XF^* formed directly by X^*-F_2 rearrangement collisions or indirectly by three-body ion-ion recombination between the positive ions X^+ produced by electron-impact ionization of $X^{(*)}$ and the negative ions F^- formed by dissociative attachment in (e-F_2) collisions. The ionization of metastable rare-gas atoms therefore plays a key role, as a mechanism for depletion of atomic metastables in the former case and as a source of production of metastable excimers via ionic recombination in the latter case.

In this paper, cross sections for the ionization of metastable Ne*, Ar*, Kr*, and Xe* by electron impact are determined as a function of the collision energy E by means of the Born approximation and the binary-encounter method which is also applied to the ionization of metastable N_2^* and CO*. It is worth noting that the corresponding theoretical treatments of electron-impact ionization of H(2s) and He(2 ^{1,3}S) yield cross sections[1] in good agreement with recent measurements.[9,10]

II. BASIC FORMULAS

The cross section for ionization of a singly excited atom B with mass M_B and ionization potential I by an incident particle A with mass M_A, speed v, and relative energy E is, in the (elastic) binary-encounter approximation given by[11,12]

$$\sigma_{nl}^I(E) = \frac{\pi}{M_{Ae}v^2}\int_I^E d\epsilon_T \int_0^\infty f_{nl}(u)\frac{du}{u}\int_{P^-}^{P^+}\frac{4}{P^4}\,\Gamma(P)\,dP, \tag{1}$$

where the distribution in speed u of the valence electron described by a spatial wave function $\phi_{nlm}(\vec{r})$ is, with all quantities in atomic units,

$$f_{nl}(u) = \frac{1}{(2l+1)} \times \sum_{m=-l}^{l}\int\left|\frac{1}{(2\pi)^{3/2}}\int\phi_{nlm}(\vec{r})e^{-i\vec{u}\cdot\vec{r}}\,d\vec{r}\right|^2 u^2\,d\hat{u} \tag{2}$$

and M_{Ae} is the reduced mass of the (A-e) binary system.

For a specified energy transfer ϵ_T to the valence electron, the momentum change P can vary between the lower limit,

$$P^- = \max[M|u'-u|, M_{AB}|v'-v|]\ ,$$
$$M = m\left(1+\frac{m}{M_i}\right),\quad M_{AB} = \frac{M_AM_B}{M_A+M_B}\ , \tag{3}$$

where m and M_i are the electronic and ionic masses, respectively, and the upper limit

$$P^+ = \min[M(u'+u), M_{AB}(v'+v)], \quad (4)$$

where the post binary-collision speeds of the projectile and target particles are, respectively,

$$v' = (v^2 - 2\epsilon_T/M)^{1/2}, \quad (5)$$

$$u' = (u^2 + 2\epsilon_T/M)^{1/2}. \quad (6)$$

In the general expression (1), the function $\Gamma(P)$, which represents the departure of the differential cross section for $(A\text{-}e)$ elastic scattering from the Rutherford value, is set to unity for direct $(e\text{-}e)$ collisions for which $M \approx M_{AB} \approx m$.

The Born approximation to the cross section for single ionization of an atom with N electrons by an incident electron can be written, with all quantities in atomic units, as

$$\sigma_{nl}^I(E) = \int_0^{\alpha(E-I)} d\epsilon \, \frac{1}{(2l+1)} \sum_{m=-l}^{l} \int \sigma_{nlm}^I(\epsilon, \hat{k}_e)\, d\hat{k}_e \quad (7)$$

in terms of the differential cross section for ejection of the electron with momentum $\vec{k}_e$ per unit solid angle and unit energy interval,

$$\sigma_{nlm}^I(\epsilon, \hat{k}_e) = \frac{8\pi}{k_i^2} \int_{K^-}^{K^+} \left| \langle \psi_f(\epsilon, \hat{k}_e; \vec{r}) | \sum_{i=1}^{N} e^{i\vec{K}\cdot\vec{r}_i} | \psi_i(n\,^3P_{0,2}; \vec{r}) \rangle \right|^2 \frac{dK}{K^3}, \quad (8)$$

where $\psi_{i,f}(\vec{r})$ are the initial and final electronic wave functions for the rare-gas atom with electronic coordinates denoted collectively by $\vec{r}$. The limits to the momentum change $(\vec{k}_i - \vec{k}_f)$ of the scattered electron are

$$K^{\mp} = (2E)^{1/2} \mp [2(E - I - \epsilon)]^{1/2}, \quad (9)$$

where the energy ϵ of ejection is $\frac{1}{2}k_e^2$ a.u. and where the kinetic energy transferred to the ion is neglected. While the parameter α in the ϵ-integration limit in (7) is unity for ionization involving distinguishable particles, Rudge and Seaton[13] have shown that, for ionization of atomic hydrogen by electrons with random spin orientations, $\alpha = 0.5$ when electron-exchange effects are fully neglected. While this choice however ensures that the faster of the scattered and ejected electrons is always described by a plane wave, neither choice is rigorously based for ionization of atoms more complex than hydrogen. The spatial wave function $\psi_i(\vec{r})$ for the initial bound metastable state of the rare-gas atom is taken as a simple product of the one-electron orbitals with quantum numbers (nlm)

$$\phi_{nlm}(\vec{r}_j) = (1/r_j) P_{nl}(r_j) Y_{lm}(\hat{r}_j), \quad j = 1, 2, \ldots, N \quad (10)$$

where the Y_{lm} are spherical harmonic functions. The corresponding wave function $\psi_f(\vec{r})$ for the final ionized state includes the orbital

$$\phi_\epsilon(\hat{k}_e; \vec{r}) = \sum_{l'=0}^{\infty} \sum_{m'=-l'}^{l'} \frac{i^{l'}}{r} e^{-i\eta_{l'}} F_{\epsilon l'}(r) \times Y_{l'm'}(\hat{r}) Y_{l'm'}^*(\hat{k}_e) \quad (11)$$

for the electron ejected in direction $\hat{k}_e$ with energy ϵ. In this study, these orbitals are obtained from a central-field approximation such that the above radial functions P_{nl} and $F_{\epsilon l}$ are appropriate solutions of the radial Schrödinger equation,

$$\frac{d^2P_{nl}(r)}{dr^2} + 2\left(E - V(r) - \frac{l(l+1)}{2r^2}\right) P_{nl}(r) = 0,$$

$$E = \begin{cases} \epsilon_{nl} < 0 \\ \epsilon > 0 \end{cases} \quad (12)$$

where the spherically symmetric interaction $V(r)$, which tends to $(-N/r)$ as $r \to 0$ and to $(-1/r)$ as $r \to \infty$ and which is frozen for all the orbitals, is determined in a manner described in the following section. All the bound and continuum orbitals therefore form an orthonormal set such that the form factor in (8) reduces to a one-electron form factor involving only the ejected electron.

The bound solutions P_{nl} to (12) are normalized to unity (for $E < 0$) and the radial continuum function behaves asymptotically as

$$F_{\epsilon l'}(r) \sim \left(\frac{2}{\pi k_e}\right)^{1/2} \sin[k_e r - (1/k_e)\ln(2k_e r) - \tfrac{1}{2}l'\pi + \eta_{l'}], \quad \text{as } r \to \infty,$$

$$\eta_{l'} = \arg\Gamma(l' + 1 - i/k_e) + \delta_{l'}(k_e), \quad (13)$$

where the additional phase shift $\delta_{l'}$ is a measure of the departure of the electron-ion interaction from pure Coulomb. The amplitude $2^{1/4}/\pi^{1/2}\epsilon^{1/4}$ is chosen so as to fulfill the normalization condition,

$$\langle \phi_\epsilon(\hat{k}_e; \vec{r}) | \phi_{\epsilon'}(\hat{k}_e'; \vec{r}) \rangle = \delta(\epsilon - \epsilon')\delta(\hat{k}_e - \hat{k}_e'), \quad (14)$$

where $\epsilon = \frac{1}{2}k_e^2$ is in atomic units such that the ionization cross section (7) is obtained by integrating (8) over $\hat{k}_e$ and ϵ. By first performing the $\hat{k}_e$ integration, it can then be shown that the differential cross section per unit ϵ is, for initial s states,

$$\sigma^{J}_{ns}(\epsilon) = \frac{8\pi}{k_i^2} \int_{K^-}^{K^+} \sum_{l'=0}^{\infty} (2l'+1) |M^{Jl'}_{\epsilon l', ns}(\epsilon, K)|^2 \frac{dK}{K^3}, \tag{15}$$

where the radial matrix element to be evaluated is

$$M^{Jl'}_{\epsilon l', ns}(\epsilon, K) = \int_0^\infty i^{-l'} e^{i\eta_{l'}} F_{\epsilon l'}(r) j_{l'}(Kr) P_{ns}(r)\, dr \tag{16}$$

in which j_l is the spherical Bessel function.

Antisymmetry of the target wave function is omitted although some account of exchange effects in the target is introduced by the use of the Hartree-Slater approximation for the interaction potential $V(r)$.

III. WAVE FUNCTIONS FOR THE RARE-GAS ATOMS

The singly excited states of rare-gas atoms, in general, follow neither the pure LS nor the jj angular momentum coupling schemes. These excited states are obtained by single excitation of one of the np outer-shell electrons of the ground-state configuration to a $n'l'$ state. The binding energy of (or effective charge seen by) this excited valence electron is substantially less than for the np electrons, and the excited electron is, on the average, relatively distant from all the core electrons, including the np-shell electrons. The spin-orbit interaction of the electrons of the atomic core can therefore be greater than the electrostatic interaction of these electrons with the excited electron and this effect manifests itself in the distinctive "core splitting" structure of the spectrum. The intermediate coupling scheme which describes the angular momentum structure is therefore closest to the pure jl (or jK) coupling wherein the orbital angular momentum $\vec{l}$ of the valence electron is coupled to the total angular momentum $\vec{j}$ of the atomic core and their resultant $\vec{K}$ is in turn coupled[14] to the valence electron spin to give the total angular momentum $\vec{J}$ of the atom.

Whatever the coupling, pure or intermediate, the total angular momentum J of the atom is a good quantum number and remains invariant under the various recoupling transformations. For the lowest excited configuration $np^5(n+1)s$, J can take the values 0, 1 (twice), and 2. Since dipole transitions within the same configuration are parity-forbidden and since the ground state is $^1S_0$, the $(np)^5(n+1)s$ states with $J=0$ and $J=2$ are therefore metastable. Expansion of these states from an intermediate coupling to a jK basis projects onto the $^2P_{1/2}[K=\frac{1}{2}]_{J=0}$ state, for $J=0$, and onto the $^2P_{3/2}[K=\frac{3}{2}]_{J=2}$ state, for $J=2$. Alternatively an expansion to an LS basis projects onto $^3P_0$ for $J=0$ and $^3P_2$ for $J=2$. Since no mixing is involved in each case, either set of pure-state notations provides convenient labeling of the metastable states. Of the remaining LS states, $^1P_1$ and $^3P_1$, the possible metastability arising from $^3P_1$ is lost by its mixing with $^1P_1$ which is dipole connected with the $^1S_0$ ground state.

In this study the effective field (potential) $V(r)$ is the same for all target electrons. Moreover the atomic core is regarded as frozen and the continuum electron moves in the same field as the initially bound excited valence electron. This potential is determined in the Hartree-Slater approximation via the following modification to the standard program of Herman and Skillman.[15] A self-consistent field (SCF) iteration for the initial excited-state configuration $[1s^22s^2\cdots np^5(n+1)s]$ yields $V_i(r)$ which when inserted in (12) provides orthonormal $P_{(n+1)s}$ and $F_{\epsilon l'}$ for a wide range of angular momentum l' (from 0 to about 30) and of energies ϵ of the ejected electron. This procedure which differs from the standard one, based on an interaction $V_0(r)$ obtained from a SCF iteration of the ground-state configuration, has been found[1] to yield considerable improvement for the helium excited states with symmetry different to that of lower-lying states. This improvement is attributed to the allowance of core relaxation whilst the symmetry condition avoids the necessity of explicit orthogonalization of the wave functions to those of lower-lying states, the ground state, in particular. In the present case the excited and ground-state configurations $np^5(n+1)s$ and np^6 are orthogonal because of the orbital angular momentum of the valence electron. As the number of atomic electrons increases, the Hartree-Slater approximation for exchange is expected to improve. On the other hand, core relaxation in the excited states diminishes whilst relativistic effects such as spin-orbit coupling, which are not included in the present treatment, become important. The same orbitals are used for the $^3P_2$ and $^3P_0$ (or $[\frac{3}{2}]_2$ and $[\frac{1}{2}]_0$) states since the major contribution to their splitting comes from spin-orbit coupling in the core,[16] an effect not included in the present treatment.

Knowledge of the bound and continuum orbitals permits evaluation of the Born radial matrix element (16) and of the speed distribution (2) for use in the binary-encounter formula (1).

Whilst preserving or introducing the following approximations of (a) omission of antisymmetry, (b) magnetic quantum-number independence of the radial orbitals $P_{nl}(r)$ and $F_{\epsilon l'}(r)$, (c) explicit $\vec{k}_e \cdot \vec{r}$ dependence of the continuum orbitals [cf. Eq. (11)]

i.e., uncoupling of the orbital angular momentum l' of the ejected continuum electron from all other angular momenta, and (d) lack of selection of the angular momentum configuration of the residual ion, one finds that the introduction of explicit coupling of the individual angular momenta (spin and orbital) of the target electrons in an intermediate, pure jK or other coupling scheme, leaves the expression (15), initially derived without coupling, unchanged.

IV. RESULTS AND DISCUSSION

A. Ionization of Ne*, Ar*, Kr*, Xe*

The ionization cross sections of metastable Ne, Ar, Kr, and Xe versus the impact energy E are displayed in Figs. 1(a)–1(d). The same cross section is assigned to the $^3P_2$ and $^3P_0$ metastable states which are treated as degenerate. The ionization potentials I used in the expressions (1), (7), and (9) are the weighted average of the potentials of the $^3P_{2,0}$ states for ionization without core transitions. The values so derived from the tables of Moore[16] are given in Table I, together with the p^5 inner-shell ionization potentials.

As the target varies from Ne* to Xe*, its physical size increases, its ionization potential decreases and the ionization cross sections exhibit the systematic increase in Figs. 1(a)–1(d). Moreover, the binary encounter curves BE drop in relation to BF, the Born cross sections obtained from integration over the full range of energy ϵ of

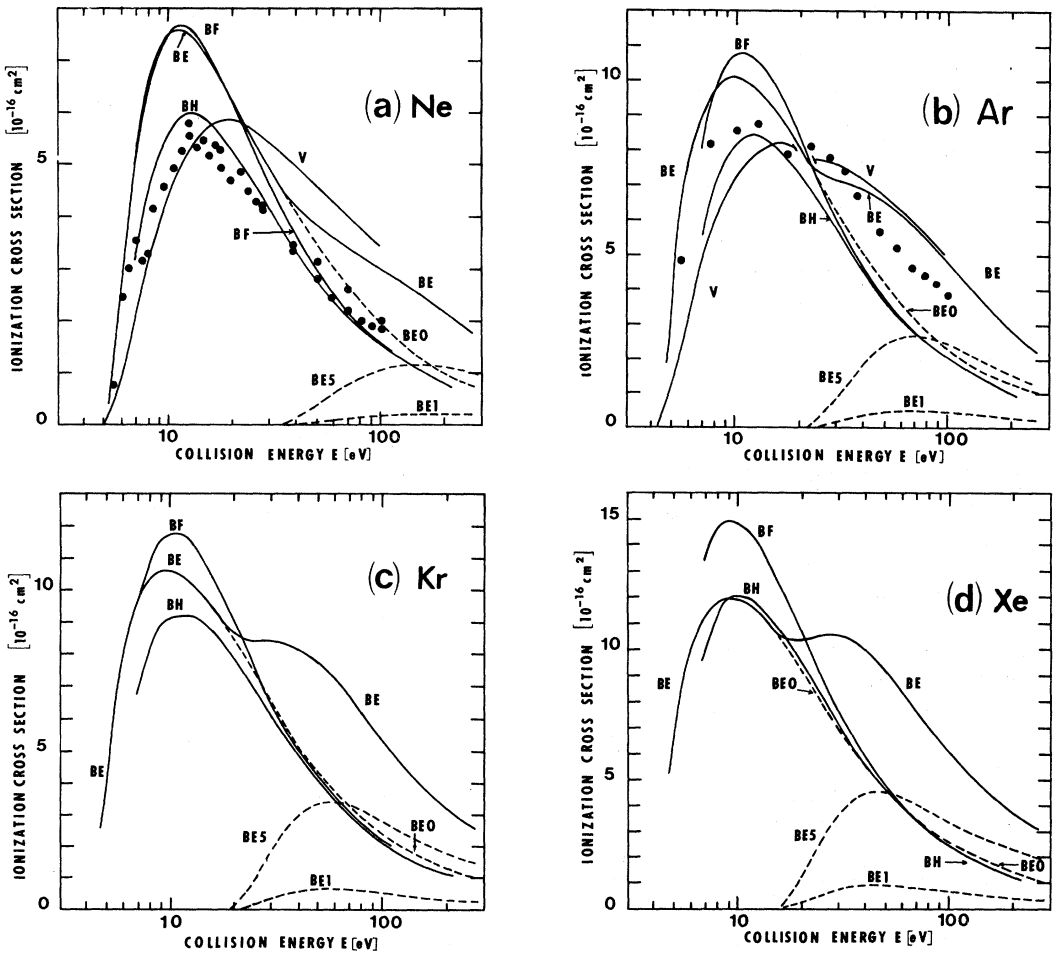

FIG. 1. Cross sections (10^{-16} cm^2) for collisional ionization of metastable (a) Ne*, (b) Ar*, (c) Kr*, and (d) Xe* by electrons with impact energy E (eV). BF and BH are the present Born results for outer-shell ionization obtained from integrations over the full and lower-half ranges of energy ϵ of the ejected electron, i.e., $\alpha = 1$ and $\frac{1}{2}$ respectively in (7) of text. The binary-encounter (quantal distribution) cross sections are denoted by BE0 for outer-shell ionization, by BE1 for ionization of one of the electrons in the np^5 shell, by BE5 for the total ionization of the np^5 shell and by BE for the sum of BE0 and BE5. Previous binary encounter (exponential distribution) results of Vriens are represented by V. ●: measurements of Dixon, Harrison, and Smith (Ref. 17).

TABLE I. Potentials I_0 and I_i for ionization of the ns outer-shell and the $(n-1)p^5$ inner-shell of metastable rare-gas atoms. $X^*(ns)$ means $X^*(1s^2, 2s^2, \ldots, (n-1)p^5, ns)$.

$X^*(ns)$	I_0 (eV)	I_i (eV)
Ne*(3s)	4.95	32.13
Ar*(4s)	4.21	20.88
Kr*(5s)	4.09	18.16
Xe*(6s)	3.44	15.41

the ejected electron, i.e., $\alpha = 1$ in (7). For example, the separation between BE and BF (which is remarkably small for He*[1] and Ne*) widens with variation of the target from Ne* to Xe* until BE eventually comes into close agreement with BH, the "half-range" Born cross sections, i.e., (7) with $\alpha = \frac{1}{2}$.

The origin of the general agreement in shape and magnitude between the binary encounter and the Born curves has already been fully investigated[1] (for the ionization of He*) and is rather instructive. For most values of the energy ϵ and the momentum change K of the ejected electron, the number of l' partial waves required for convergence of the matrix element (16) or form factor with respect to l', the angular momentum of the ejected electron, is relatively small, 9 or less. However, for large ϵ, the required number increases sharply near the Bethe ridge defined by

$$K_{BR}^2 = 2(I+\epsilon) = 2\epsilon_T \qquad (17)$$

where a "resonance" can occur between $F_{\epsilon l'}$ and $j_{l'}$ in (16) and where up to 30 partial waves are required for convergence. Moreover, for low ϵ, the s-d,f (i.e., $l'=2,3$) transitions dominate (16). As ϵ is increased, the dominant transition shifts from s-d,f to s-g, s-h, etc., for those K near the Bethe ridge where a broad distribution of (16) over l' is exhibited. For large ϵ, these contributions maximize with respect to K in the vicinity of the Bethe ridge. These properties can be interpreted[1] mainly in terms of the spatial range of the wave function of the initial excited state, and of the drift of both the final continuum orbital $F_{\epsilon l'}(r)$ and Bessel function $j_{l'}(Kr)$ out of this range. The overall agreement between the Born and the binary-encounter curves originates from the resulting closeness between the Born and the binary encounter determinations[11] of the form factor squared in (8) away from the optical $K \to 0$ limit. The impact energies for which the ionization cross section is relatively large involves momentum transfers K for which the form factor requires many partial waves and is substantial. This situation, where many partial waves and therefore multipoles are required, is generally well described by the binary-encounter method.

Also shown in Fig. 1 is the binary-encounter contribution arising from the p^5 inner-shell, obtained by multiplying the ionization cross section for ejection of a single p electron by the occupation number of the p^5 shell. The outer valence electron remains in its initial excited state. Again, as the target varies from Ne* to Xe*, the inner-shell ionization potentials drops, the inner-shell ionization cross section increases in magnitude, absolute as well as relative to the outer-shell ionization cross section, and its effect on the shape of the excitation (ionization) function becomes more prominent by the display of a secondary maximum.

The results for ionization of Ne* and Ar* are compared with the experimental data of Dixon *et al.*[17] Whereas the measurements are in better agreement with the Born full-range calculations[1] for ionization of He($2\,^3S$) the experimental data for ionization of Ne* and Ar* are in closer agreement with the (lower) Born half-range calculations than with the Born full-range results. The data for Ar* support the increasing importance of p^5 inner-shell ionization. Dixon *et al.*[10] have subjected their measurements of ionization of He($2\,^3S$) to a correction for systematic effects arising from charge exchange reactions occurring in the experimental collision region. This correction, if applicable to the data for Ne* and Ar*, is not included in the data shown here in Figs. 1(a) and 1(b); however the correction is appreciable only at impact energies greater than 100 eV, a range which is beyond that of the experimental data shown here.

Also shown for completeness are previous binary-encounter calculations of Vriens,[18] based however on an exponential velocity distribution which is at variance[19] with any proper quantal distribution, such as the one used here.

B. Bethe plots

The calculations and experimental data for ionization of Ne*, Ar*, Kr*, and Xe* are also presented in Figs. 2(a)–2(d) in the form of Bethe plots ($\sigma^I E$ versus $\log_{10} E$) which emphasize the behavior in the intermediate and near-asymptotic energy range.

These plots show that the slopes of the Born curves for outer-shell ionization of metastable Ne, Ar, Kr, and Xe at impact energies beyond 100 eV are quite small in comparison with, say, that[1] for outer-shell ionization of He($2\,^3S$) (cf. Fig. 4 of Ref. 1) thereby indicating that the outer-shell photoionization cross sections of metastable Ne,

Ar, Kr, and Xe are substantially smaller than the corresponding cross section of He($2\,^3S$) over an appreciable range of ejected electron energy beginning from threshold. Thus, a reversal, between target He($2\,^3S$) on one hand, and metastable Ne, Ar, Kr, and Xe targets on the other, occurs in the magnitudes of the cross sections depending on whether the outer-shell ionization is caused by electron impact or by photon impact. However, the effective photoionization cross section also involves the contribution from the contiguous inner shell; for Ne*–Xe* the inner shell (p^5) has five electrons instead of one for He($2\,^3S$) and it begins to contribute at lower impact energies.

For the heavy rare gases the E^{-1} asymptotic dependence (instead of the correct $E^{-1}\log_{10}E$) of the ionization cross section normally exhibited in the binary encounter approximation does not appear until $E \gtrsim 1$ keV. This late onset, combined with the weakness of the dipole transition oscillator strength discussed earlier, corresponds to the fact that the binary encounter curves for outer-shell ionization remains above the Born curve BF as the impact energy becomes large, instead of crossing below as implied by the asymptotic dependence (cf. Figs. 1 and 2).

While there is reasonable accord between the Bethe plots associated with the theoretical and experimental results at low energies when only ionization of the outer-shell occurs, the Fig. 2, in contrast to Fig. 1, clearly shows that any measure of agreement between the asymptotic slopes is ob-

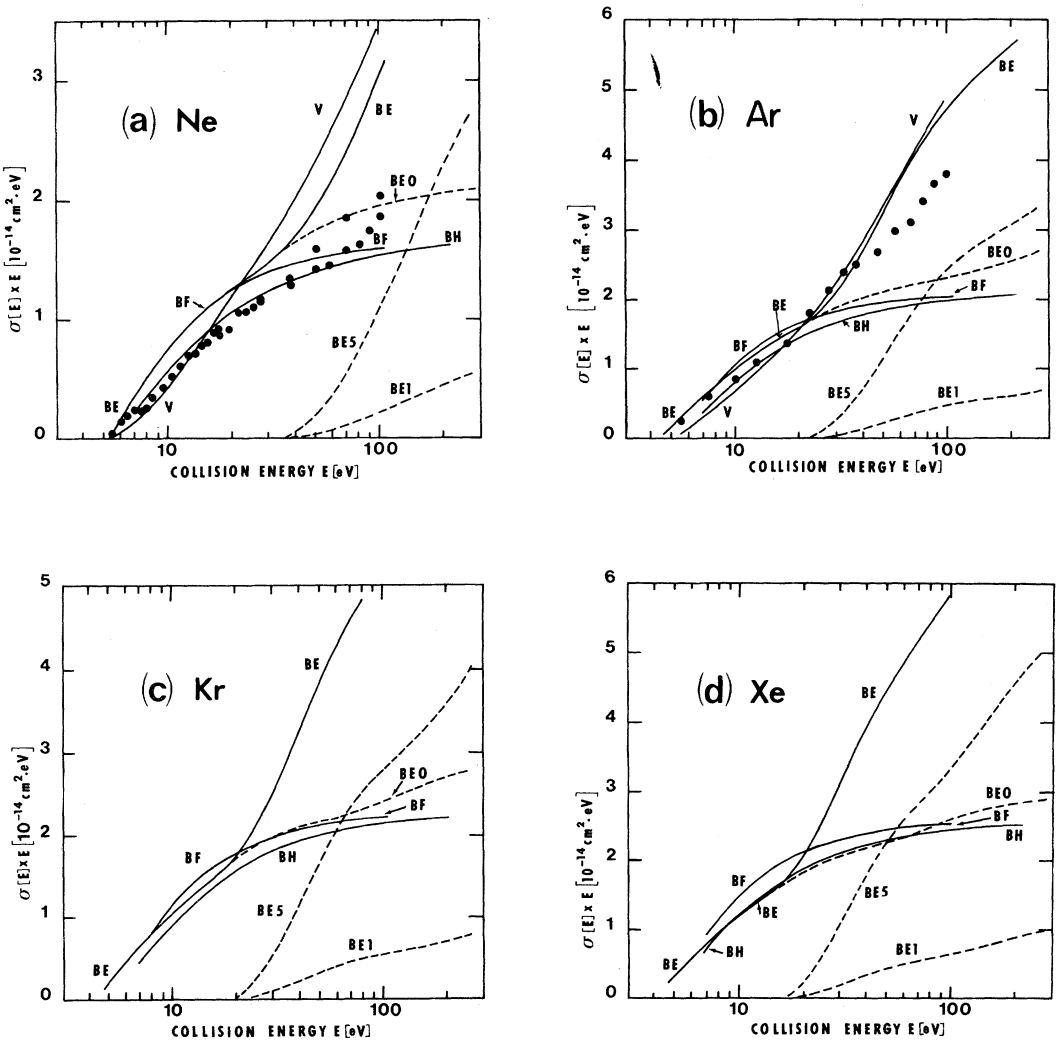

FIG. 2. Bethe plots (cross section times collision energy E versus $\log_{10}E$) for electron-impact ionization of metastable (a) Ne*, (b) Ar*, (c) Kr*, and (d) Xe*. Labeling of curves as in Fig. 1.

tained only by inclusion of the p^5 inner-shell contributions, especially for Ar*. These inner-shell contributions are adequately described[1] by the binary-encounter method and for Kr* and Xe*, become larger and increasingly important at the lower impact energies.

C. Tabulation

The numerical values of the electron-impact ionization cross section of Ne*, Ar*, Kr*, and Xe* calculated in the full-range and half-range Born approximations (for ionization from the outer shell alone) and in the binary-encounter approximation (with and without the inner-shell contributions) are given in Tables II and III. Measurements for electron-impact ionization of Kr* and Xe* are not available; the binary-encounter results inclusive of p^5 shell contributions or, for $E \lesssim 20$ eV, the Born half-range results, should provide reasonable estimates of the cross sections of Kr* and Xe*.

We have not considered multiple processes such as double ionization or ionization with simultaneous excitation. In relation to single processes, multiple processes are small for a He target (~1%) but are less so for heavier rare gases with larger occupation numbers and lower excitation energies (see for instance Schmidt *et al.*[20]). For a precise comparison between theory and experiment, one should include these multiple processes fully in the calculations or else ensure that they do not contribute to the measurements.

D. Ionization of metastable N_2 and CO

Ionization of diatomic molecules like N_2 and CO in metastable states is also important for gas laser dynamics. We have therefore applied the binary-encounter approximation of Sec. II to the electron-impact ionization of N_2 in the $A\,^3\Sigma_u^+$ and $a'\,^1\Sigma_u^-$ metastable states and of CO in the $a\,^3\Pi$ metastable state.

The electronic configurations of the metastable states of N_2 and CO as well as those of the low-lying states of N_2^+ and CO^+ are shown in Table IV. It shall be assumed that single processes, involving only one target electron, are more important than multiple processes requiring multielectron target transitions. This assumption also makes the ionization problem tractable within the framework of the binary-encounter approximation of Sec. II; otherwise, inclusion of multiple processes would require consideration of energy exchange with the residual ion. We shall therefore restrict ourselves to consideration of the following single-process transitions:

$$e + N_2(A\,^3\Sigma_u^+) \rightarrow 2e + N_2^+(A\,^2\Pi_u) \quad (I = 10.79 \text{ eV}) , \tag{18}$$

$$e + N_2(a'\,^1\Sigma_u^-) \rightarrow 2e + N_2^+(A\,^2\Pi_u) \quad (I = 8.56 \text{ eV}) , \tag{19}$$

$$e + CO(a\,^3\Pi) \rightarrow 2e + CO^+(X\,^2\Sigma^+) \quad (I = 8.2743 \text{ eV}) . \tag{20}$$

The molecular orbitals used are the orbitals previously derived by Richardson[21] for N_2^+ and Huo[22]

TABLE II. Born (full-range, BF; half-range, BH) and binary encounter (BE) cross sections (in units of 10^{-16} cm^2) for the ionization of the outer-shell of metastable Ne*($2p^5 3s$) and Ar*($3p^5 4s$) by electrons with energy E (a.u.). The cross sections BEI include additional inner-shell contributions as determined from the binary-encounter approximation.

	Ne*				Ar*			
E (a.u.)	BF	BH	BE	BEI	BF	BH	BE	BEI
0.25	4.56	3.14	4.73	4.73	7.98	5.53	8.73	8.73
0.30	6.46	4.65	6.61	6.61	9.79	7.18	9.87	9.87
0.35	7.34	5.45	7.39	7.39	10.67	8.05	10.11	10.11
0.40	7.68	5.84	7.59	7.59	10.79	8.37	9.99	9.99
0.50	7.46	5.98	7.35	7.35	10.34	8.33	9.46	9.46
0.75	8.82	5.22	6.18	6.18	8.21	7.17	7.94	7.94
1.25	4.13	3.77	4.55	4.57	5.44	5.07	5.71	7.05
2	2.75	2.57	3.25	3.74	3.59	3.38	3.90	6.40
3	1.90	1.83	2.34	3.26	2.44	2.40	2.73	5.35
4	1.46	1.41	1.81	2.92	1.88	1.84	2.13	4.47
6	...	0.971	1.24	2.47	...	1.25	1.52	3.31
8	...	0.741	0.949	2.06	...	0.951	1.20	2.64

TABLE III. Born (full-range, BF; half-range, BH) and binary encounter (BE) cross sections (in units of 10^{-16} cm^2), for the ionization of the outer-shell of metastable Kr*($4p^5 5s$) and Xe*($5p^5 6s$) by electrons with energy E (a.u.). The cross sections BEI include additional inner-shell contributions as determined from the binary-encounter approximation.

	Kr*				Xe*			
E (a.u.)	BF	BH	BE	BEI	BF	BH	BE	BEI
0.25	9.54	6.69	9.48	9.48	13.19	9.56	11.09	11.09
0.30	10.99	8.26	10.46	10.48	14.70	11.38	11.85	11.85
0.35	11.67	9.12	10.66	10.66	14.86	12.03	11.95	11.95
0.40	11.74	9.19	10.50	10.50	14.61	12.02	11.77	11.77
0.50	11.11	9.11	9.96	9.96	13.56	11.32	11.09	11.09
0.75	8.82	7.81	8.34	8.60	10.44	9.37	9.08	10.40
1.25	5.85	5.45	5.91	8.35	6.83	6.32	6.25	10.41
2	3.91	3.63	4.01	7.44	4.47	4.23	4.25	8.74
3	2.63	2.58	2.84	5.97	3.02	2.97	3.07	6.81
4	2.01	1.97	2.24	4.89	2.32	2.26	2.43	5.63
6	•••	1.31	1.60	3.64	•••	1.52	1.71	4.29
8	•••	1.02	1.25	2.96	•••	1.17	1.31	3.48

for CO*, who used Slater-type-orbital (STO) bases. [Similar orbitals have also been calculated by Rose and McKoy[23] using Gaussian-type-orbital (GTO) bases.] Hence, the appropriate Fourier transforms are obtained and averaged over angles as in (2) to give the initial speed distribution $f(u)$. Although a spherical distribution may be a poor approximation because of the molecular axis, the effects of rotation and random orientation of the molecular target partially offset this inadequacy. The ionization potentials used in (1) for each molecular orbital are the vertical ionization potentials derived from the data of Gilmore[24] for N_2 and Krupenie[25] for CO, at the equilibrium internuclear distance of the initial state, even though the molecular orbital may have been derived at the nuclear separation of the ground state. The cross sections for the ionization processes (18)–(20) at impact energies below 200 eV are shown in Fig. 3.

Since Richardson[21] gives the same $1\pi_g$ orbital for $N_2(A\,^3\Sigma_u^+)$ and $N_2(a'\,^1\Sigma_u^-)$, expression (1) adopts the same speed distribution for these two states. The only difference arises from the ionization potentials and the main effect is a reduction in the magnitude of the ionization cross section.

On the other hand, $N_2(a'\,^1\Sigma_u^-)$ and $CO(a\,^3\Pi)$ have very similar potentials for single-process ionization. Any slight differences between the curves

TABLE IV. Electronic configurations for N_2^*, N_2^+, CO*, CO^+.

Configuration[a]	$(1\sigma_g)^2$	$(1\sigma_u)^2$	$(2\sigma_g)^2$	$(2\sigma_u)^i$	$(1\pi_u)^j$	$(3\sigma_g)^k$	$(1\pi_g)^l$
$N_2\ X\,^1\Sigma_g^+$				$i=2$	$j=4$	$k=2$	$l=0$
$A\,^3\Sigma_u^+$				2	3	2	1
$a'\,^1\Sigma_u^-$				2	3	2	1
$N_2^+\ X\,^2\Sigma_g^+$				2	4	1	0
$A\,^2\Pi_u$				2	3	2	0
$B\,^2\Sigma_u^+$				1	4	2	
				2	3	1	1

Configuration[b]	$(1\sigma)^2$	$(2\sigma)^2$	$(3\sigma)^2$	$(4\sigma)^i$	$(1\pi)^j$	$(5\sigma)^k$	$(2\pi)^l$
$CO\ X\,^1\Sigma^+$				$i=2$	$j=4$	$k=2$	$l=0$
$a\,^3\Pi$				2	4	1	1
$CO^+\ X\,^2\Sigma^+$				2	4	1	
$A\,^2\Pi$				2	3	2	
$B\,^2\Sigma^+$				1	4	2	

[a] Cf. Gilmore, Ref. 24.
[b] Cf. Krupenie, Ref. 25.

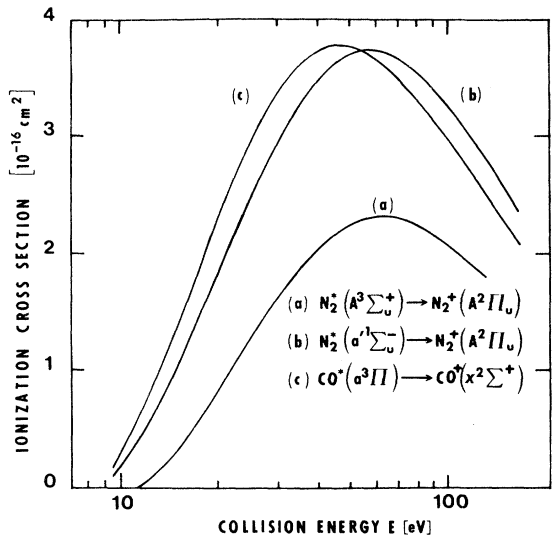

FIG. 3. Binary-encounter cross sections (10^{-16} cm^2), (a), (b), and (c), for the ionization of metastable $N_2^*(A\,^3\Sigma_u^+)$, $N_2^*(a'\,^1\Sigma_u^-)$, and $CO^*(a\,^3\Pi)$, respectively, by electrons with energy E (eV). The final state of the residual ion is indicated.

for ionization of $N_2(a'\,^1\Sigma_u^-)$ and $CO(a\,^3\Pi)$ are therefore attributed to differences between the $1\pi_g$ orbital of N_2^* and the 2π orbital of CO*. Any similarity between the properties of N_2 and CO usually originates from the isoelectronic character of these molecules, while any difference arises from the heteronuclear aspect.

While the ground states of N_2 and CO have similar electronic configurations, $N_2^*(a'\,^1\Sigma_u^-)$ and $CO^*(a\,^3\Pi)$—and for that matter $N_2^+(A\,^2\Pi_u)$ and $CO^+(X\,^2\Sigma^+)$—have slightly different electronic configurations. However, since the binary encounter method of Sec. II relies mainly on the properties of the valence electron ($1\pi_g$ or 2π), the difference between the configurations of the remaining electrons is reflected only indirectly through its effect on the valence electron ($1\pi_g$ or 2π).

Metastable N_2 and CO have greater ionization potentials than metastable rare gases and have correspondingly smaller electron-impact ionization cross sections as seen by comparing Fig. 1 with Fig. 3.

V. CONCLUSION

Electron-impact ionization cross sections of $[np^5(n+1)s]$ metastable Ne, Ar, Kr, and Xe have been calculated in the Born and the binary-encounter approximations. The further approximations used here make explicit coupling of the target angular momenta—to reflect the peculiarities of the heavy rare-gas spectra—unnecessary.

As the atomic number of the target increases, the cross section for ionization from the outer shell increases. Ionization of the inner p^5 shell also becomes increasingly important with increasing target complexity. Moreover the binary-encounter results drop in relation to the Born results.

The maximum of the experimental data of Dixon *et al.*[17] is in fair agreement with that of the Born half-range calculations. Beyond the maximum the inner-shell contribution becomes evident. The Bethe plots suggest that the outer-shell photoionization cross sections of metastable Ne, Ar, Kr, and Xe are overall smaller than that of He($2\,^3S$).

The binary-encounter approximation has also been used for the single-process ionization of the π valence electron of metastable N_2 and CO. Their greater ionization potentials lead to cross sections smaller than for He*, Ne*, Ar*, Kr*, and Xe*.

*Research sponsored by the Air Force Propulsion Laboratory, Air Force Systems Command, USAF under Contract No. F33615-76-C-2003 and by US-ERDA under contract E-(40-1)-5002/7.

[1]D. Ton-That, S. T. Manson, and M. R. Flannery, J. Phys. B (to be published).
[2]J. J. Ewing and C. A. Brau, Appl. Phys. Lett. 27, 350 (1975); 27, 435 (1975); Phys. Rev. A 12, 129 (1975); J. Chem. Phys. 63, 4640 (1975).
[3]C. P. Wang, H. Mirels, D. G. Sutton, and S. N. Suchard, Appl. Phys. Lett. 28, 326 (1976).
[4]R. Burnham, N. W. Harris, and N. Djeu, Appl. Phys. Lett. 28, 86 (1976).
[5]E. R. Ault, R. S. Bradford, Jr., and M. L. Bhaumik, Appl. Phys. Lett. 27, 413 (1975).
[6]J. E. Velazco and D. W. Setser, J. Chem. Phys. 62, 1990 (1975).
[7]M. F. Golde, J. Mol. Spectros. 58, 261 (1975).
[8]J. Tellinghuisen, J. M. Hoffman, G. C. Tisone, and A. K. Hays, J. Chem. Phys. 64, 2484 (1976).
[9]A. J. Dixon, A. von Engel, and M. F. A. Harrison, Proc. R. Soc. London A 343, 333 (1975).
[10]A. J. Dixon, M. F. A. Harrison, and A. C. H. Smith, J. Phys. B 9, 2617 (1976). See also Ref. 17.
[11]L. Vriens, *Case Studies in Atomic Collision Physics I*, edited by E. W. McDaniel and M. R. C. McDowell (North-Holland, Amsterdam, 1969), p. 337.
[12]M. R. Flannery, J. Phys. B 4, 892 (1971).
[13]M. R. H. Rudge and M. J. Seaton, Proc. Roy. Soc. London A 283, 262 (1965).
[14]I. I. Sobel'man, *Introduction to the Theory of Atomic Spectra* (Pergamon, New York, 1972), Chap. 3, Sec. 10.6, p. 53 and Chap. 5, Sec. 20.5–7, pp. 185–193.
[15]F. Herman and S. Skillman, *Atomic Structure Calcu-*

lations (Prentice-Hall, Englewood Cliffs, N. J., 1963).
[16]C. E. Moore, *Atomic Energy Levels*, NBS Circ. No. 467 (U.S. GPO, Washington, D.C., 1949), Vol. I.
[17]A. J. Dixon, M. F. A. Harrison, and A. C. H. Smith, *Abstracts of Papers of Eighth International Conference on the Physics of Electronic and Atomic Collisions*, edited by B. C. Cobic and M. V. Kurepa (Institute of Physics, Belgrade, Yugoslavia, 1973), Vol. 1, p. 405; and private communication.
[18]L. Vriens, Phys. Lett. 8, 260 (1964).
[19]A. Burgess and I. C. Percival, *Advances in Atomic and Molecular Physics* (Academic, New York, 1968), p. 124.
[20]V. Schmidt, N. Sandner, and H. Kuntzemüller, Phys. Rev. A 13, 1743 (1976).
[21]J. W. Richardson, J. Chem. Phys. 35, 1829 (1961).
[22]W. M. Huo, J. Chem. Phys. 45, 1554 (1966).
[23]J. B. Rose and V. McKoy, J. Chem. Phys. 55, 5435 (1971).
[24]F. R. Gilmore, J. Quant. Spectrosc. Radiat. Transfer 5, 369 (1965).
[25]P. H. Krupenie, *The Band Spectrum of Carbon Monoxide* NSRDS-NBS 5 (U.S. GPO, Washington, D.C., 1966).